K. D. E. Kerrouche, A. Mezouar, L. Boumediene, A. Van Den Bossche

A comprehensive review of LVRT capability and sliding mode control of grid-connected wind-turbine-driven doubly fed induction generator

In this paper, a comprehensive review of several strategies applied to improve the Low Voltage Ride-Through (LVRT) capability is presented for grid-connected wind-turbine-driven Doubly Fed Induction Generator (DFIG). Usually, the most proposed LVRT solutions in the literature based on: hardware solutions, which increase the system costs and software solutions, which increase the control system complexity. Therefore, the main objective of this study is to take into account grid requirements over LVRT performance under grid fault conditions using software solution based on Higher Order-Sliding Mode Control (HOSMC). Effectively, this control strategy is proposed to overcome the chattering problem and the injected stator current harmonics into the grid of the classical First Order Sliding Mode (FOSMC). Furthermore, the resultant HOSMC methodology is relatively simple; where, the online computational cost and time are considerably reduced. The LVRT capacity and effectiveness of the proposed control method, compared to the conventional FOSMC, are validated by time-domain simulation studies under Matlab on a 1.5 MW wind-turbine-driven DFIG.

Key words: Wind turbine, DFIG, LVRT, HOSMC, FOSMC.

Sveobuhvatan pregled LVRT mogućnosti i kliznog režima upravljanja vjetroagregata spojenog na mrežu s dvostruko napajanim asinkronim generatorom. U ovom radu, prikazan je sveobuhvatan pregled strategija primjenjenih za poboljšanje sposobnosti rada tijekom prolaznih smetnji niskog napona mreže za vjetroagregat s dvostruko napajanim asinkronim generatorom (DFIG). Uobičajeno, većina predloženih LVRT rješenja u literaturi temelji se na: hardverskim rješenjima, što povećava troškove sustava i softverskih rješenja te složenost sustava upravljanja. Stoga je glavni cilj ovog istraživanja da se uključuje i zahtjevi mreže kroz ponašanje LVRTa u uvjetima mrežnih kvarova korištenjem softverskog rješenja zasnovanoga na kliznom režimu rada višeg reda (HOSMC). Efektivno, ova upravljačka strategija je predložena kako bi se prevladali oscilacije i ubacivanje harmonika struje statora u mrežu klasičnim metodama kliznog režima rada prvog reda (FOSMC). Nadalje, rezultantna metodologija HOSMC je relativno jednostavna; gdje su online računski zahtjevi i potrebno vrijeme značajno smanjeni. LVRT kapacitet i učinkovitost predložene metode upravljanja, u usporedbi s konvencionalnim FOSMC potvrđene su simulacijama u vremenskoj domeni u Matlabu na 1.5 MW vjetroagregatu s DFIG-om.

Ključne riječi: Vjetroagregat, DFIG, LVRT, HOSMC, FOSMC.

1 INTRODUCTION

Induction generators, especially Doubly Fed Induction Generators (DFIG) are used a lot in Wind Energy Conversion Systems (WECS) application [1], [2]. Simple induction generators have some weaknesses such as reactive power absorption and uncontrolled voltage during variable rotor speed. These problems are solved by installation of DFIG and power electronic converter or controllers [3], [4]. The particular feature of the DFIG is that the generated power by the rotor converter is only a small part from the total provided power with its stator directly connected to the utility grid [5], [6] and [7]. Therefore, the

size, the cost and losses of the power converter are smaller compared to a full size power converter. When the stator and rotor of DFIG are both connected to the grid, Low Voltage Ride-Through (LVRT) capability is considered as a primordial challenge in wind turbines design [8]. LVRT requires wind turbines to remain connected to the power system during grid voltage dips. Therefore, many research papers focus on studying the dynamic response of wind farms during and after the clearance of the fault without disconnection from the grid.

In [9], the effects of voltage drops caused by faults on DFIG's to overcome grid fault conditions are studied.
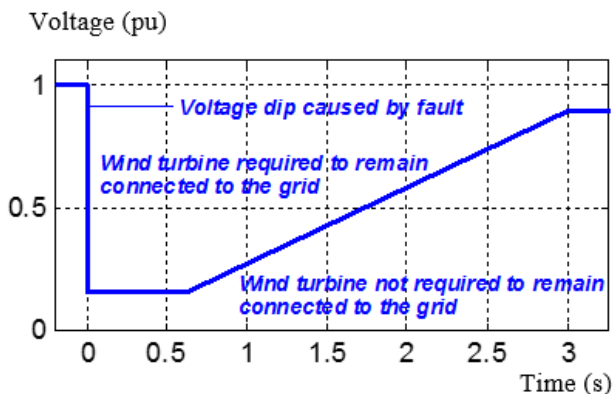
Fig. 1: Operating voltage range for WECS.

A classical controller: Proportional–Integral (PI) was designed for the control techniques of DFIG when grid faults occur like during voltage dips [10] and unbalanced grid voltages [11]. LVRT control of wind turbines with DFIGs under symmetrical voltage dips is dealt in [8]. In [12], a control scheme for limiting the dc-link voltage fluctuation has been applied to the Grid Side Converter (GSC). However, the performance of the DFIG depends on the appropriate choice of the PI gains, which the optimization of gains takes a lot of time [13, 14]. Thereby, if the controllers have bad performances in systems with DFIG driven by wind turbine, the quality and the quantity of the generated power can be influenced. A hybrid current control scheme was introduced in [15], implemented in the Rotor Side Converter (RSC) and GSC of DFIG, to enhance low and high voltage ride-through capabilities of DFIG-based wind turbines. A control technique of the GSC is proposed in [16], in order to direct the rotor power flow during grid fault conditions. Rotor current controller based on adaptive internal model control is designed in [17]; with different adjustment mechanisms similar to Lyapunov theory, fuzzy and adaptive neuro-fuzzy inference system to improve the voltage sag ride through. One of the most important matters involved in WECS improvement is linked to the inclusion of new robust control strategies, based on low computational time, cost algorithms capable of optimizing the system efficiency, while, reducing structural loading.

The present paper can be seen as a continuation of the above-mentioned works. An overview of the recently published LVRT schemes is discussed. Then, in the second part, this study focuses attention on the improvement of a method, which allows better performances of the whole system under study, using LVRT software solution based on Lyapunov theory. The main contribution of this study is to test the High Order Sliding Mode Control (HOSMC) based on Super-Twisting Algorithm (STA) to ensure the DFIG controllability under symmetrical voltage drop. The

grid code considered in this work is similar to that of E.ON [19], as shown in Fig.1.

2   AN OVERVIEW FOR DFIG LVRT SOLUTIONS

In the previous circumstances, the WECSs were intended to be disconnected during the grid fault conditions and any Low Voltage Ride-Through (LVRT) solutions were considered. In [20] an overview of the latest research about the LVRT is provided for wind turbine based DFIG. Generally, the state of art for DFIG LVRT solutions are categorized as seen in Fig.2.

The hardware solutions:

In [21] an overview of some solutions of the LVRT capability development is shown for different types of WECSs based on fault protection schemes. [22] Shows an overview of internal protection systems of WECSs based DFIG. In [23] a novel protection scheme for transient rotor current is suggested to improve the performance of DFIG under grid fault. In [24] a proposed protection strategy for DFIG, which incorporates a series-dynamic-resistor, a dc-link chopper and a crowbar with a synchronised switching control.

In [9, 25], a Flexible AC Transmission System (FACTS) device such as Static Synchronous Compensator (STATCOM) is proposed to improve the LVRT ability for wind generation systems based DFIG. In [26] a FACTS system based STATCOM for DFIG to alleviate the effects of grid faults is proposed. In [27, 28] a FACTS device connected in series with the grid called Dynamic Voltage Restorer (DVR) to mitigate the effect of the voltage drop in the electrical grid under fault conditions is suggested. In [29] the use of DVR for enhancement of DFIG LVRT is investigated.

The software solutions:

In [30] an overview of studies issues related to modeling, analysis and advanced control of LVRT of wind turbines with DFIG is presented. In [31] a comprehensive review about LVRT techniques and controllers for different wind generation systems is shown. In [32] a study of the coupling between excitation control and the electromagnetic method for DFIG under symmetric grid fault condition is proposed. In [33, 34] a vector-based hysteresis current controller for LVRT competence improvement of DFIG is presented. In [20] a modified VC to fulfil the LVRT requirements from the distribution or transmission electrical grid is discussed.

In [35] a novel LVRT software solution based dual-sequence decomposition method to diminish the oscillations and improve the DFIG's LVRT ability during unbalanced electrical grid is suggested. In [36] a fuzzy logic controller is synthetized for wind generation based DFIG
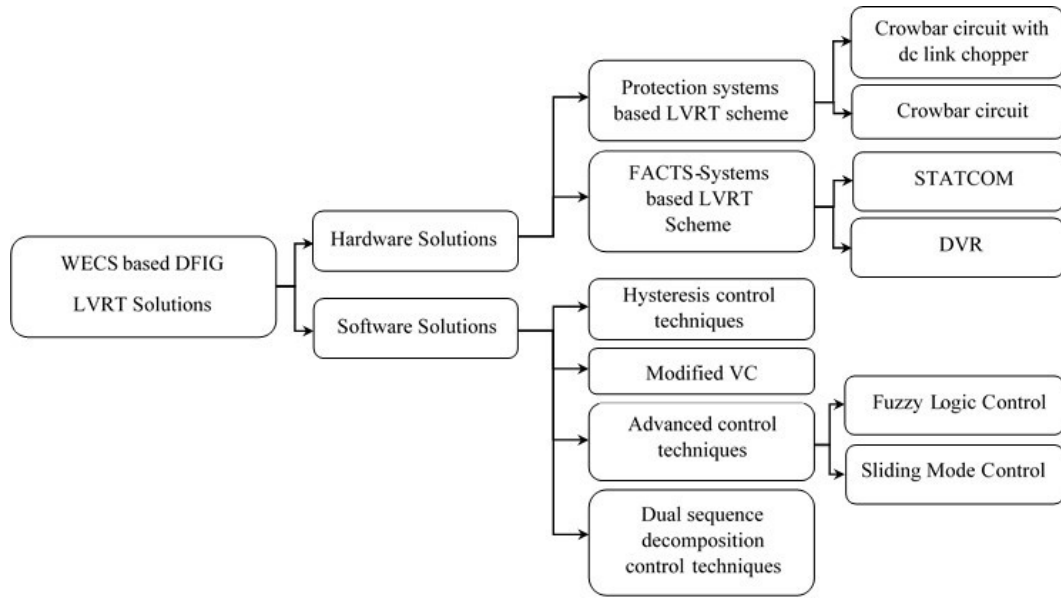
Fig. 2: Categories of the LVRT solutions for the WECS based DFIG.

under electrical grid fault conditions. In [18, 51] sliding mode control for DFIG LVRT competence enhancement is investigated.

3 DFIG MODELLING

Based on the assumption of linear magnetic circuits, the stator and rotor voltages expressions of the DFIG under balanced operating condition can be written as follows [37, 38]:

$$\overline{V_s} = \begin{bmatrix} v_{ds} \\ v_{qs} \end{bmatrix} = \begin{bmatrix} R_s\, i_{ds} + \frac{d\phi_{ds}}{dt} - \omega_s\, \phi_{qs} \\ R_s\, i_{qs} + \frac{d\phi_{qs}}{dt} + \omega_s\, \phi_{ds} \end{bmatrix} \quad (1)$$

$$\overline{V_r} = \begin{bmatrix} v_{dr} \\ v_{qr} \end{bmatrix} = \begin{bmatrix} R_r\, i_{dr} + \frac{d\phi_{dr}}{dt} - (\omega_s - \omega)\, \phi_{qr} \\ R_r\, i_{qr} + \frac{d\phi_{qr}}{dt} + (\omega_s - \omega)\, \phi_{dr} \end{bmatrix} \quad (2)$$

Where i_{ds}, i_{qs}, i_{dr} and i_{qr} are, respectively, the direct and quadrature stator and rotor currents. R_s and R_r are stator and rotor resistances. ω_s, ω are stator and rotor electrical angular speeds, with $\omega = p \cdot \Omega_g$, p is the pair pole number.

The stator and rotor fluxes can be expressed as:

$$\overline{\phi_s} = \begin{bmatrix} \phi_{ds} \\ \phi_{qs} \end{bmatrix} = \begin{bmatrix} L_s\, i_{ds} + M\, i_{dr} \\ L_s\, i_{qs} + M\, i_{qr} \end{bmatrix} \quad (3)$$

$$\overline{\phi_r} = \begin{bmatrix} \phi_{dr} \\ \phi_{qr} \end{bmatrix} = \begin{bmatrix} L_r\, i_{dr} + M\, i_{ds} \\ L_r\, i_{qr} + M\, i_{qs} \end{bmatrix} \quad (4)$$

Where L_s, L_r and M are stator, rotor and mutual inductances.

The active and reactive powers at the stator are defined as:

$$\begin{cases} P_s = v_{ds}\, i_{ds} + v_{qs}\, i_{qs} \\ Q_s = v_{qs}\, i_{ds} - v_{ds}\, i_{qs} \end{cases} \quad (5)$$

The principle of this technique is based on stator flux orientation in such a way that the stator flux vector is aligned into d-axis [38, 39]. This approach is achieved by setting the quadrature component of the stator flux to the null value:

$$\phi_s = \phi_{ds} \ \Rightarrow \ \phi_{qs} = 0 \quad (6)$$

Using the condition mentioned above and the neglected per phase stator resistance, which is a convincing approximation for WECS grid connected, the voltages can be deduced as:

$$\begin{cases} v_{ds} = 0 \\ v_{qs} = \omega_s \phi_s = V_s \end{cases} \quad (7)$$

When replacing the rotor flux (4) in (2) and using the above condition (7), the rotor voltages become:

$$\begin{cases} v_{dr} = \sigma L_r \frac{di_{dr}}{dt} + R_r i_{dr} - \sigma L_r \omega_r i_{qr} \\ v_{qr} = \sigma L_r \frac{di_{qr}}{dt} + R_r i_{qr} + \sigma L_r \omega_r i_{dr} + \omega_r \frac{M}{L_s} \phi_s \end{cases} \quad (8)$$

Where V_s the stator voltage magnitude is assumed constant, $\omega_r = \omega_s - \omega = g\,\omega_s$ is the slip frequency, g is the slip range and $\sigma = 1 - \frac{M^2}{L_s\, L_r}$ is the leakage coefficient. Accordingly, with regard to (6), the fluxes are simplified as specified below:

$$\begin{cases} \phi_{ds} = L_s i_{ds} + M i_{dr} \\ 0 \ = L_s i_{qs} + M i_{qr} \end{cases} \quad (9)$$

From Eq. (9), the stator currents can be deduced as:

$$\begin{cases} i_{ds} = \frac{\phi_{ds} - M i_{dr}}{L_s} \\ i_{qs} = -\frac{M}{L_s} i_{qr} \end{cases} \tag{10}$$

By using (5), (6) and (10), the stator active and reactive powers can then be expressed only versus these rotor currents as:

$$\begin{cases} P_s = -V_s \frac{M}{L_s} i_{qr} \\ Q_s = -V_s \frac{M}{L_s} \left(i_{dr} - \frac{\phi_s}{M} \right) \end{cases} \tag{11}$$

4 DFIG CONTROL STRATEGY

This section shows the design of the Sliding Mode Control (SMC) based on Lyapunov application. The sliding surface specifies the relative degree of a system, and, therefore, the order of the applicable SMC [40, 41, 42 and 46]. As the system is of first-order relative degree in grid connected, it may be controlled applying First-Order Sliding Mode Control (FOSMC) or High-Order Sliding Mode Control (HOSMC) [43, 44]. The synthesis of the two SMCs is detailed in subsequent sections.

4.1 First Order Sliding Mode Control

Since the optimal power tracking control method is applied to define the reference of the active power, the first-order sliding surfaces representing the error between the measured powers and their references can be expressed as follows:

$$S_{dq} = \begin{bmatrix} S_d(Q_s) \\ S_q(P_s) \end{bmatrix} = \begin{bmatrix} e(Q_s) \\ e(P_s) \end{bmatrix} \tag{12}$$

Where $e(Q_s) = Q_s^* - Q_s$ and $e(P_s) = P_s^* - P_s$. Then, their derivatives are:

$$\dot{S}_{dq} = \begin{bmatrix} \dot{S}_d(Q_s) \\ \dot{S}_q(P_s) \end{bmatrix} = \begin{bmatrix} \dot{Q}_s^* - \dot{Q}_s \\ \dot{P}_s^* - \dot{P}_s \end{bmatrix} \tag{13}$$

Substituting the expression of powers of (11) in (13), the derivatives of sliding surfaces become:

$$\dot{S}_{dq} = F_1 + D_1 V_r \tag{14}$$

Where

$$F_1 = \begin{bmatrix} \dot{Q}_s^* + \\ V_s \frac{M}{\sigma L_r L_s}(-R_r i_{dr} + \sigma L_r \omega_r i_{qr}) - V_s \frac{\phi_s}{L_s} \\ \dot{P}_s^* + \\ V_s \frac{M}{\sigma L_r L_s}\left(-R_r i_{qr} - \sigma L_r \omega_r i_{dr} - \omega_r \frac{M}{L_s}\phi_s\right) \end{bmatrix} \tag{15}$$

$$D_1 = \frac{M}{\sigma L_r L_s} \begin{bmatrix} V_s & 0 \\ 0 & V_s \end{bmatrix}, \overline{V_r} = \begin{bmatrix} v_{dr} & v_{qr} \end{bmatrix}^T \tag{16}$$

The stability Lyapunov theory is used to verify the zero-convergence of the sliding surfaces, by satisfying the following condition:

$$\dot{V} = S^T \dot{S} < 0 \tag{17}$$

Considering the structure of (2), the following control law derives the applied rotor voltage:

$$\overline{V_r} = \begin{bmatrix} v_{dr} \\ v_{qr} \end{bmatrix} = \begin{bmatrix} v_{dr,eq} + v_{dr,n} \\ v_{qr,eq} + v_{qr,n} \end{bmatrix} \tag{18}$$

Where $[v_{dr,eq}, v_{qr,eq}]^T$ is the equivalent control and $[v_{dr,n}, v_{qr,n}]^T$ is the switching part of the control. The equivalent control terms, are derived by letting $\dot{S}_{dq} = 0$ [45]. Taking into account the equivalent and switching part, the control law (18) becomes:

$$\overline{V_r} = \begin{bmatrix} v_{dr} \\ v_{qr} \end{bmatrix} = \tag{19}$$
$$-D_1^{-1} F_1 - D_1^{-1} \begin{bmatrix} a_Q & 0 \\ 0 & a_P \end{bmatrix} \begin{bmatrix} sign(S_d(Q_s)) \\ sign(S_q(P_s)) \end{bmatrix}$$

Where $a_Q > 0$ and $a_P > 0$,

$$\begin{bmatrix} v_{dr,eq} \\ v_{qr,eq} \end{bmatrix} = \tag{20}$$
$$\begin{bmatrix} -\frac{\sigma L_r L_s}{M V_s} \dot{Q}_s^* + R_r i_{dr} - \sigma L_r \omega_r i_{qr} + \frac{\sigma L_r}{M}\phi_s \\ -\frac{\sigma L_r L_s}{M V_s} \dot{P}_s^* + R_r i_{qr} + \sigma L_r \omega_r i_{dr} + \frac{\omega_r M}{L_s}\phi_s \end{bmatrix}$$

The FOSMC described in this work ensures the fast tracking of the instantaneous active and reactive powers exchanged between the DFIG and the grid. However, fast switching may generate an undesirable chattering effect, which may excite unmodeled high-frequency system transients, inject broad band harmonics into the grid and even result in unexpected instability [47, 48 and 51].

4.2 High Order Sliding Mode Control

As an attractive solution to the FOSMC, a High-Order Sliding-Mode Control (HOSMC) is adopted in this paper.

The second order sliding surfaces are defined as follows:

$$S_{dq} = \begin{bmatrix} S_d(Q_s) \\ S_q(P_s) \end{bmatrix} = \begin{bmatrix} e(Q_s) + b_Q \int e(Q_s) \\ e(P_s) + b_P \int e(P_s) \end{bmatrix} \tag{21}$$

Considering the derivative of (21) and by substituting the expression of powers of (11), the derivatives of sliding surfaces become:

$$\dot{S}_{dq} = F_2 + D_2 V_r \tag{22}$$

Where

$$F_2 = \begin{bmatrix} \dot{Q}_s^* - \frac{V_s}{L_s}\left(b_Q\,\phi_s - i_{dr}\,M\left(\frac{R_r}{\sigma L_r} - b_Q\right) - \right. \\ \left. M\omega_r i_{qr}\right) + b_Q\,Q_s^* \\ \dot{P}_s^* + \frac{V_s\,M}{L_s}\left(i_{qr}\left(b_P - \frac{R_r}{\sigma L_r}\right) - \right. \\ \left. \omega_r i_{dr} - \frac{\omega_r M}{\sigma L_r L_s}\phi_s\right) + b_P\,P_s^* \end{bmatrix}$$

(23)

$$D_2 = \frac{M}{\sigma\,L_r\,L_s}\begin{bmatrix} V_s & 0 \\ 0 & V_s \end{bmatrix}, V_r = \begin{bmatrix} v_{dr} & v_{qr} \end{bmatrix}^T$$

(24)

In order to confirm the zero-convergence of the sliding surfaces, the same condition of Lyapunov theory (17) can be also used. From the structure of (22) and (23), the rotor voltage V_r is derived according to the following control law:

$$\overline{V}_r = \begin{bmatrix} v_{dr} \\ v_{qr} \end{bmatrix} = \begin{bmatrix} v_{dr,eq} + v_{dr,ST} \\ v_{qr,eq} + v_{qr,ST} \end{bmatrix}$$

(25)

By letting $\dot{S}_{dq} = 0$, the equivalent control is derived as follows:

$$\begin{bmatrix} v_{dr,eq} \\ v_{qr,eq} \end{bmatrix} = -D_2^{-1}F_2$$

(26)

From (26), (23) and (24), the following expression is obtained:

$$\begin{bmatrix} v_{dr,eq} \\ v_{qr,eq} \end{bmatrix} = \begin{bmatrix} -\frac{\sigma L_r L_s}{M V_s}\left(\dot{Q}_s^* + b_Q\left(Q_s^* - Q_s\right)\right) + \\ R_r\,i_{dr} - \sigma\,L_r\omega_r i_{qr} \\ -\frac{\sigma L_r L_s}{M V_s}\left(\dot{P}_s^* + b_P\left(P_s^* - P_s\right)\right) + \\ R_r\,i_{qr} + \sigma\,L_r\omega_r i_{dr} + \frac{\omega_r M}{L_s}\phi_s \end{bmatrix}$$

(27)

Details of Lyapunov approach based on Supper-Twisting Algorithm (STA) have been presented in [48, 49]. It should be regarded that the STA is notably designed by two parts; one ensuring that sliding surface $\dot{S}_{dq} = 0$ is achieved in finite time, another related to the integral of the switching variable sign [47, 50 and 51]. The STA given by [42] can be written as:

$$\begin{bmatrix} v_{dr,ST} \\ v_{qr,ST} \end{bmatrix} = \begin{bmatrix} c_Q \sqrt[\gamma]{|S(Q_s)|}sign(S(Q_s)) + \\ d_Q \int sign(S(Q_s))\,dt \\ c_P \sqrt[\gamma]{|S(P_s)|}sign(S(P_s)) + \\ d_P \int sign(S(P_s))\,dt \end{bmatrix}$$

(28)

Where $\gamma = 1/2$ to guarantee the real second order sliding mode and c_P, c_Q and d_P, d_Q are positive gains. Substituting the control law (25), (27) and (28) into the derivative of sliding surfaces (22) gives:

$$\dot{S}_{dq} = \frac{-M V_s}{\sigma L_r L_s}\begin{bmatrix} c_Q \sqrt{|S_d(Q_s)|}sign\,(S_d(Q_s)) + \\ d_Q \int sign\,(S_d(Q_s))\,dt \\ c_P \sqrt{|S_q(P_s)|}sign\,(S_q(P_s)) + \\ d_P \int sign\,(S_q(P_s))\,dt \end{bmatrix}$$

(29)

Admitting that $sgn(s) = s/|s|$, the time derivatives of (29) becomes:

$$\ddot{S}_{dq} = -\frac{M V_s}{\sigma\,L_r\,L_s}\begin{bmatrix} \frac{c_Q}{2\sqrt{|S(Q_s)|}}\dot{S}(Q_s) + d_Q\frac{S(Q_s)}{|S(Q_s)|} \\ \frac{c_P}{2\sqrt{|S(P_s)|}}\dot{S}(P_s) + d_P\frac{S(P_s)}{|S(P_s)|} \end{bmatrix}$$

(30)

Assuming that $|S(Q_s)| = \delta_Q$ and $|S(P_s)| = \delta_P$, when the sliding regime is reached, these gains are close to zero. Using the expression of sliding surfaces in (21), the following expression can be rewritten from Eq. (30):

$$\begin{cases} \ddot{e}(P_s) + \left(b_P + \frac{c_P M V_s}{2\sigma\,L_r\,L_s\sqrt{\delta_p}}\right)\dot{e}(P_s) \\ \quad + \frac{M V_s}{\sigma\,L_r\,L_s\sqrt{\delta_p}}\left(\frac{1}{2}b_p c_P + \frac{d_p}{\sqrt{\delta_p}}\right)e(P_s) \\ \quad + \frac{b_p\,d_p\,M V_s}{\sigma\,L_r\,L_s\delta_p}\int e(P_s) = 0 \\ \ddot{e}(Q_s) + \left(b_Q + \frac{c_Q M V_s}{2\sigma\,L_r\,L_s\sqrt{\delta_Q}}\right)\dot{e}(Q_s) \\ \quad + \frac{M V_s}{\sigma\,L_r\,L_s\sqrt{\delta_Q}}\left(\frac{1}{2}b_Q c_Q + \frac{d_Q}{\sqrt{\delta_Q}}\right)e(Q_s) \\ \quad + \frac{b_Q\,d_Q\,M V_s}{\sigma\,L_r\,L_s\delta_Q}\int e(Q_s) = 0 \end{cases}$$

(31)

Taking the time derivative of (31), the third-order differential equations of the error dynamics are:

$$\begin{cases} \dddot{e}(P_s) + \alpha_1\ddot{e}(P_s) + \alpha_2\dot{e}(P_s) + \alpha_3 e(P_s) = 0 \\ \dddot{e}(Q_s) + \alpha_1\ddot{e}(Q_s) + \alpha_2\dot{e}(Q_s) + \alpha_3 e(Q_s) = 0 \end{cases}$$

(32)

Therefore, once δ_P, δ_Q are fixed the STA is tuned by an adequate selection of $b_P, b_Q, c_P, c_Q, d_P, d_Q$, through the following third-order characteristic equation:

$$\begin{aligned} \left(s^2 + 2\,\xi\,\omega_0\,s + \omega_0^2\right)\left(s + k\,\xi\,\omega_0\right) = \\ s^3 + \underbrace{(2+k)\,\xi\,\omega_0}_{\alpha_{1t}}s^2 + \underbrace{\left(1 + 2\,k\,\xi^2\right)\omega_0^2}_{\alpha_{2t}}s + \underbrace{k\,\xi\,\omega_0^3}_{\alpha_{3t}} \end{aligned}$$

(33)

Where s is Laplace operator, k is high gain- $k > 10$-, conducts to a pair of dominant poles with respect to a third one placed at $s = -k\,\xi\,\omega_0$. Hence, it can be taken into account that the error dynamics are absolutely defined through ξ damping coefficient and ω_0 natural frequency. Considering that $\alpha_1 = \alpha_{1t}, \alpha_2 = \alpha_{2t}$ and $\alpha_3 = \alpha_{3t}$ expressions for α_1, α_2 and α_3 provided in (32), as well as those for α_1, α_2 and α_{3t} considered in (33), the latter three conditions give the following equations:

$$\begin{cases} b_P^3 - (2+k)\,\xi\,\omega_0\,b_P^2 + \\ \quad \left(1 + 2\,k\,\xi^2\right)\omega_0^2\,b_P - k\,\xi\,\omega_0^3 = 0 \\ b_Q^3 - (2+k)\,\xi\,\omega_0\,b_Q^2 + \\ \quad \left(1 + 2\,k\,\xi^2\right)\omega_0^2\,b_Q - k\,\xi\,\omega_0^3 = 0 \end{cases}$$

(34)

$$\begin{cases} c_P = \frac{2\sigma L_s L_r}{M V_s}\sqrt{\delta_p}\left[(2+k)\,\xi\,\omega_0 - b_P\right] \\ c_Q = \frac{2\sigma L_s L_r}{M V_s}\sqrt{\delta_Q}\left[(2+k)\,\xi\,\omega_0 - b_Q\right] \end{cases}$$

(35)

$$\begin{cases} d_P = \frac{\sigma L_s L_r}{M V_s} \delta_p \, k \, \xi \, \omega_0^3 \\ d_Q = \frac{\sigma L_s L_r}{M V_s} \delta_p \, k \, \xi \, \omega_0^3 \end{cases} \qquad (36)$$

It is worth mentioning that the coefficients in (34) coincide with those of (33), excepting the negative signs of the squared and the autonomous terms. The three values for b_P, b_Q are equal to the poles of characteristic (33), while their real parts have opposite signs. The real parts of the chosen poles must essentially be negative to guarantee the stability of the studied system. Figure 3 shows the block diagram of the HOSMC scheme for DFIG.

5   SIMULATION RESULTS

Grid voltage faults could induce a high transient current into the rotor circuit, which may breakdown the power converters and result in disconnection of DFIG wind turbines from the power network. Henceforth, the grid fault mitigation is becoming a more challenging problem for wind power farms with uninterrupted injected power. Wherefore, in this section, some simulations are done in order to analyze only the influence of the grid fault condition on the dynamic behavior of the generator.

Fig.4 shows the block diagram of the vector control scheme for DFIG based on HOSMC/FOSMC, which is designed in the Simulink environment. In this simulation, wind speed varies from $8.9\,\text{m/s}$ to $7.8\,\text{m/s}$ as shown in Fig. 5. At $1.5\,\text{s}$ the positive-sequence voltage drops to $40\,\%$ for a time of $0.5\,\text{s}$, as shown in Fig. 6a.

The SPWM module is used in order to generate the IGBT gate control signals to drive the IGBT converter. The switching frequency of converter is set to $1\,\text{kHz}$; the nominal DC converter is set to $2000\,\text{V}$. A Phase-Locked-Loop (PLL) estimates the frequency, the grid voltage magnitude and the stator angle. The accurate estimation of these variables is necessary for both control strategy and grid connection. All the simulations have been elaborated with a fixed-step size of $0.5\,\text{ms}$ in order to consider digital implementation in future works. In practice, the controllers' parameters are never determined according to inequalities. Therefore, the suitable technique is to adapt the controller parameters during computer simulations. Furthermore, theses simulations are done in order to compare between two approaches HOSMC and FOSMC in sensibility to external perturbations (grid fault conditions). The system quantities are labelled in per-unit notation. The parameters of the WECS are reported in Appendix A.

It can be clearly observed from Fig.5b, that during the period of the grid voltage drop, there are fluctuations in the generator speed with using FOSMC compared with that of HOSMC.

The stator angle tracking is shown in Fig. 6b. It is noticed that the variations of grid voltage do not cause change

in voltage angle. The reactive power produced by the generator is controlled at $0\,\text{pu}$. Indeed, the unity power factor is guaranteed at the stator side, by maintaining the reactive power at zero. Fig.7a, b show the active and reactive stator powers. As can be seen, the presence of oscillations in the occurrence of the fault. It is realized from these figures, that that the dynamic response of the generator, during voltage dip, when controlled with the HOSMC is improved compared with that obtained when the generator is controlled with the FOSMC. The responses react quickly with less overshoots. Further, the steady state error after the clearance of fault is eliminated when the HOSMC is applied. The constant power behavior can support the grid during voltage sag. In Fig.8a, b, the errors of stator active and reactive powers with HOSMC and FOSMC are displayed. It can be seen, that during and after the grid fault, the control policy with HOSMC has a good performance against external disturbances and chattering is significantly reduced.

Fig.9a, b show the stator currents of the generator; it is clear that the frequency of the stator currents is the same as that of the grid. For comparison, the transient behavior of DFIG with conventional FOSMC shown in Fig.9a, where it can be noticed that this control is not capable to suppress the current overshoots at the stator winding to around $1.644\,\text{pu}$. In the other hand, it is clearly indicated that with the proposed HOSMC, the stator currents are reduced to around $0.8793\,\text{pu}$ and may not exceed their tolerable limits and without triggering the protective devices. Figs. 10 and 11, respectively, give the stator current harmonic spectra under normal and fault conditions for different control strategies. Obviously, conventional FOSMC results in higher stator current harmonic distortion than that from proposed HOSMC.

It is distinct from Fig.12b, that the proposed HOSMC is capable to reduce peak transient rotor currents to around $0.889\,\text{pu}$ avoiding the tripping of the RSC, while the value for the FOSMC is about $1.417\,\text{pu}$ (Fig.10a). In addition, it is clearly shown in the figures that compared with FOSMC, the current transient period of the proposed HOSMC scheme decays faster and lasts only in the fault period.

The amplitude of the stator flux is constant at the steady-state and rotates synchronously with the grid voltage. Instantly after the apparition of the voltage drop, forced and natural flux components will be induced in the stator flux. During voltage drop, the forced component is rotating with the grid frequency; afterward, the natural flux is static with the stator.

Fig. 13a, b show the trajectory of the stator flux. Before the voltage sag, the stator flux traces a circle with radius equal to $1\,\text{pu}$. The flux of the stator with HOSMC is very well centered compared with that obtained with FOSMC.
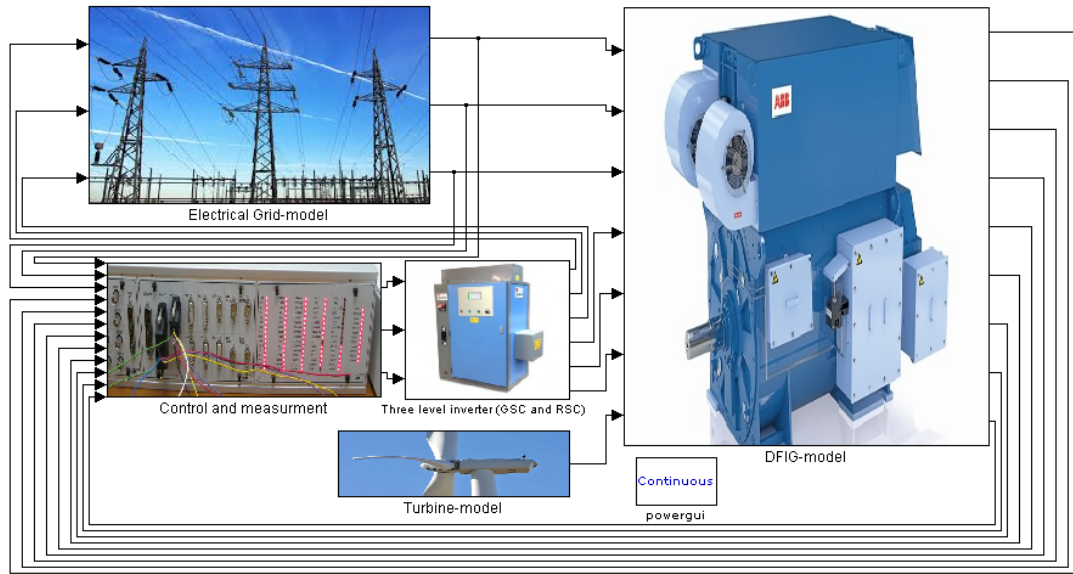
Fig. 3: Block diagram of HOSMC scheme for DFIG.

When the voltage sag starts, the circle radius decreases as the diminution of the voltage and the center of the circle is displaced accordingly to the natural component of the stator flux [52]. After the clearance of the voltage sag, the natural component of the stator flux is attenuated and the trajectory of the stator flux becomes centered again. However, it is noticed from these figures that compared with HOSMC, the stator flux trajectory of the FOSMC scheme is not well centered with an important transitory and slowly decays. The rotor flux in Fig.14a, b show ripples superimposed on its circular trajectory due to the frequency switching of PWM.

6   CONCLUSION

The most challenging problem for Doubly Fed Induction Generator (DFIG) wind turbines grid-connected is to inject

uninterrupted electrical power with grid faults mitigation. Hence, high transient rotor currents could be induced by these faults, which may breakdown the power converters and the disconnection of DFIG from the electrical grid. Therefore, in this paper, two categories of Low Voltage Ride Trough (LVRT) solutions, i.e., hardware and software are comprehensively reviewed. Among the suggested approaches in literature, the cost of applying software solutions is lower than most of the hardware approaches.

According to the developed review, this paper, presents software LVRT solution with an advanced control technique of stator powers, exchanged between the DFIG and the grid, based on stator flux orientation and Lyapunov theory designed. This proposed control strategy based on High Order Sliding Mode Control (HOSMC) must mitigate the effects of control action on the system structure and the produced power quality, while maintaining accept-

Fig. 4: Simulink block diagram of the wind-turbine-driven DFIG.
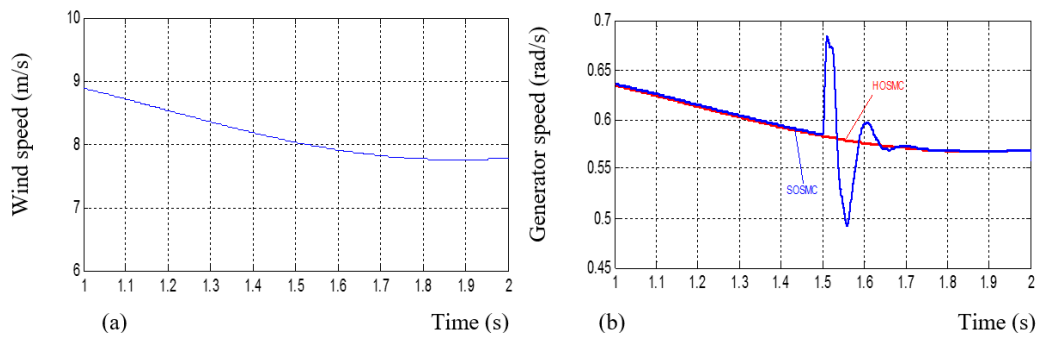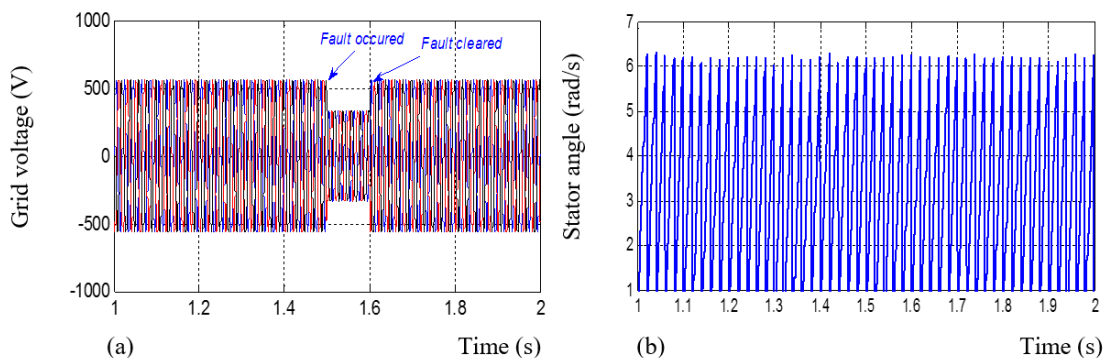

Fig. 5: (a) Wind speed, (b) Generator speed.

Fig. 6: (a) Grid voltage, (b) Stator angle

able performance during voltage sags.

Through simulations, the proposed control scheme has been proved suitable for this WECS application. The HOSMC has shown better LVRT performance and reliability than First Order Sliding Mode Control (FOSMC), practically, the absence of chattering phenomenon with an
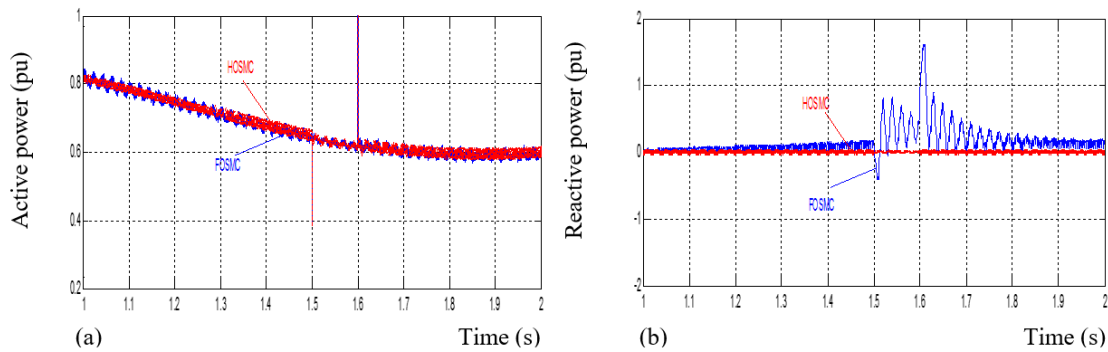
Fig. 7: (a) Stator active power with HOSMC and FOSMC, (b) Stator reactive power with HOSMC and FOSMC
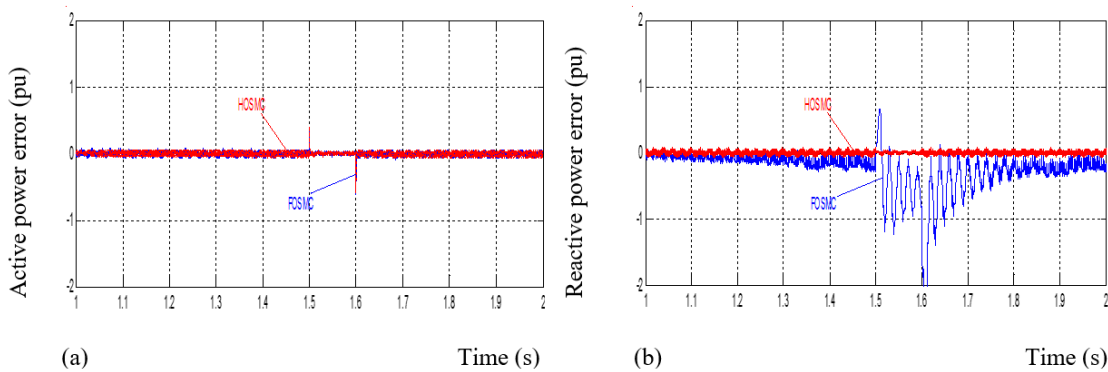
Fig. 8: (a) Errors of stator active power with HOSMC and FOSMC, (b) Errors of stator reactive power with HOSMC and FOSMC
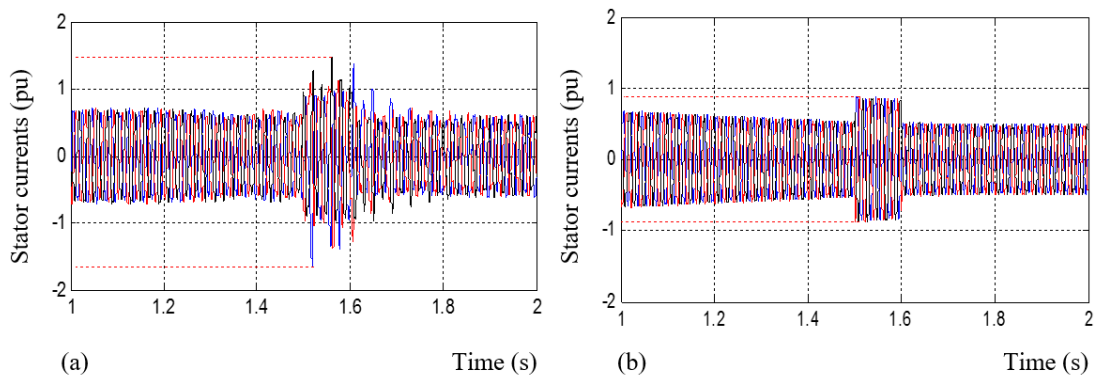
Fig. 9: Stator currents: (a) with FOSMC, (b) with HOSMC

ameliorated system stability. It can also be demonstrated that HOSMC approach can protect the generator against harmful over-currents in the rotor windings when grid voltage dips, and then the life time of mechanical and electrical systems is prolonged without significantly increasing the complexity of the LVRT software solution. Moreover, the particular attractive feature of the control law approach designed following this HOSMC, compared with FOSMC, is

the smoothness of the converter firing angle and providing less harmonics in stator currents into the grid during normal and fault conditions with a reduced chattering. All the computer simulations have been designed with a fixed-step size of 0.5 ms in order to consider digital implementation at experimental validation in future works.

In this part, simulations are investigated with a 1.5 MW generator connected to a 690V/50 Hz grid [53]. The pa-
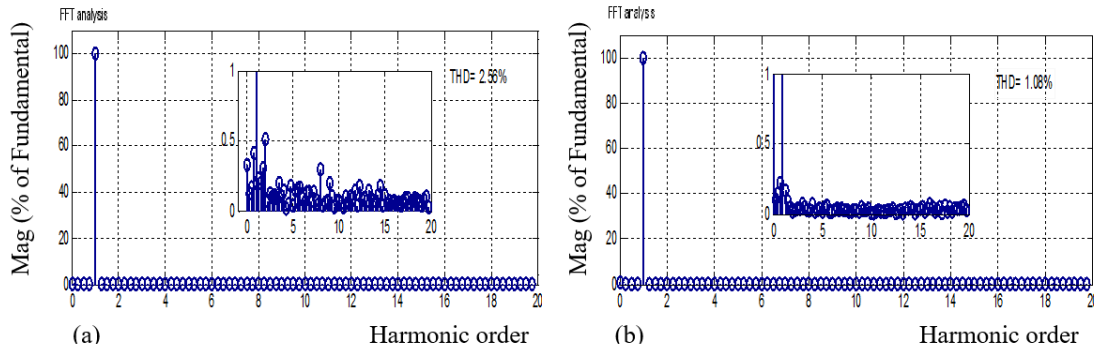
Fig. 10: Harmonic spectra of the injected stator currents during normal condition: (a) with FOSMC, (b) with HOSMC
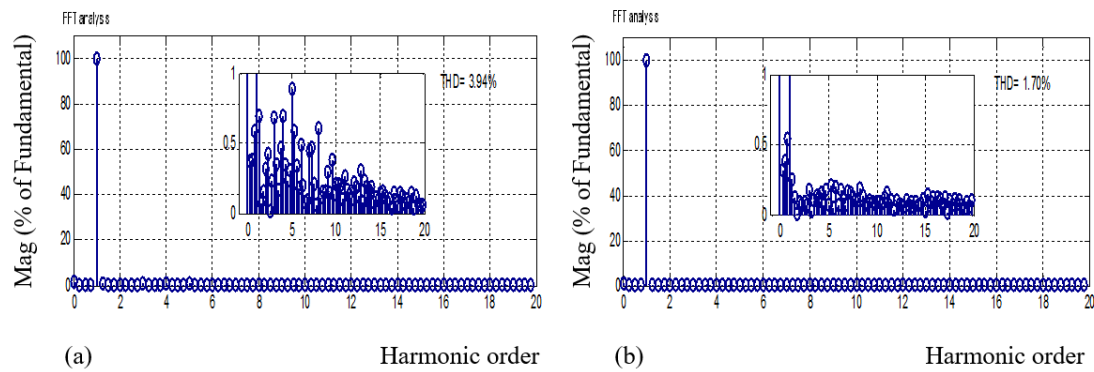

Fig. 11: Harmonic spectra of the injected stator currents during fault condition: (a) with FOSMC, (b) with HOSMC
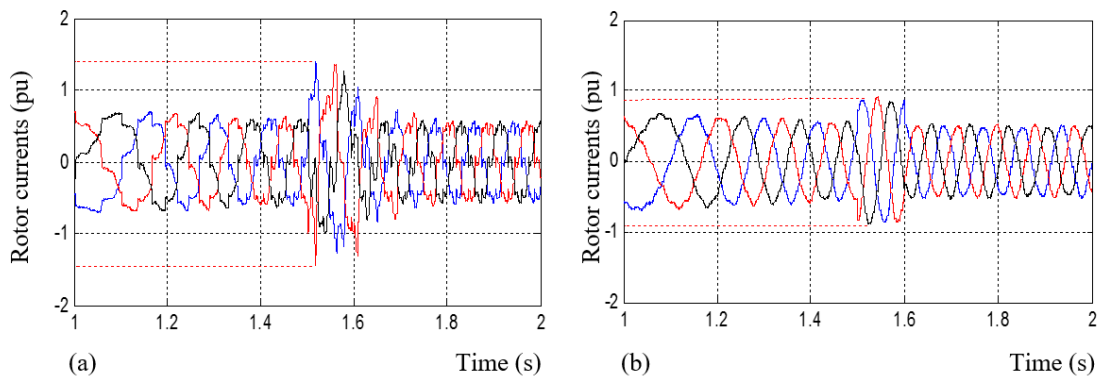

Fig. 12: Rotor currents: (a) with FOSMC, (b) with HOSMC.

rameters of the turbine and the generator are presented in the table below.

ACKNOWLEDGEMENTS

REFERENCES

[1] A. A. B. M.Zin, M. P.HA, A. B.Khairuddin, L.Jahanshaloo, O.Shariati, "An overview on doubly fed induction generators controls and contributions to wind based electricity generation,"*Renewable and Sustainable Energy Reviews*, vol. 27, pp. 692-708, 2013.

[2] M.Mohseni, S. M.Islam, "Review of international grid codes for wind power integration: Diversity, technology and
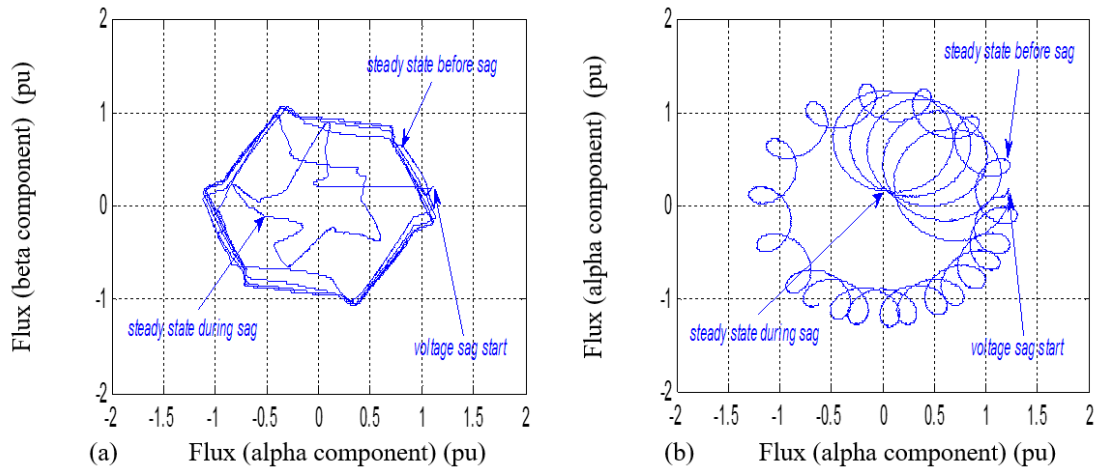
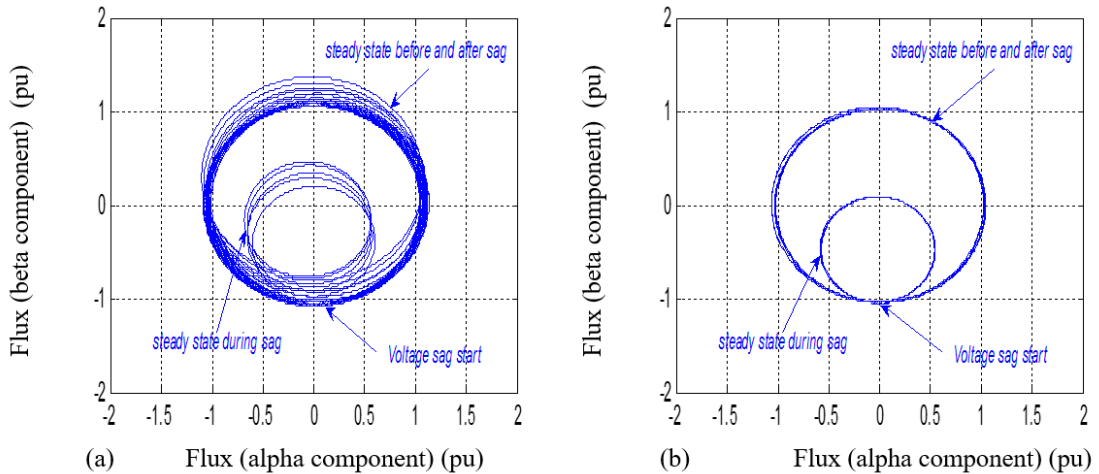Fig. 13: Stator flux trajectory: (a) with FOSMC, (b) with HOSMC.

Fig. 14: Rotor flux trajectory: (a) with FOSMC, (b) with HOSMC.

Parameters	values
Turbine	
number of blades	3
turbine radius	35.25 m
Gear box ratio	90
DFIG	
Power	1.5 MW
Nominal voltage	690 V
Frequency	50 Hz
Number of poles pair	2
Stator resistance	$0.012\,\omega$
Rotorique resistance	$0.021\,\omega$
Stator inductance	0.0137 H
Rotor inductance	0.01367 H
Mutual inductance	0.0135 H
(Turbine+DFIG)	
Generator inertia	1000 Kg.m2
Friction factor	0.0024 Kg.m/s

a case for global standard," *Renewable and Sustainable Energy Reviews*, vol. 16, pp. 3876-3890, 2012.

[3] M.Tazil, V.Kumar, R. C.Bansal,S. Kong, Z. Y. Dong, W. Freitas, et al, "Three-phase Doubly Fed Induction Generators: an overview," *IET Journal on Electric Power Applications*, vol. 4, pp. 75-89, 2010.

[4] G.Tsourakisa,B. M.Nomikosb, C. D. Vournasa, "Effect of wind parks with doubly fed asynchronous generators on small-signal stability,"*Electric Power Systems Research*, vol. 79, pp. 190-200, 2009.

[5] M.Abdelhafidh, M. O.Mahmoudi, L.Nezli, O. Bouchhida, "Modeling and Control of a Wind Power Conversion System Based on the Double-Fed Asynchronous Generator,"*International Journal of Renewable Energy Research*

(IJRER), vol. 2, no 2, pp. 300-306, 2012.

[6] K.Kerrouche, A. Mezouar, K. Belgacem, "Decoupled Control of Doubly Fed Induction Generator by Vector Control for Wind Energy Conversion System," *Energy procedia*, vol. 42, pp. 239-248, 2013.

[7] Z. Wang, Y. Sun, G. Li, BT. Ooi, "Magnitude and frequency control of grid-connected doubly fed induction generator based on synchronised model for Wind power generation,"*IET Journal on Renewable Power Generation*, vol. 4, pp. 232-41, 2010.

[8] A.Rolan, J. Pedra, F. Corcoles, "Detailed study of DFIG-based wind turbines to overcome the most severe grid faults,"*Electrical Power and Energy Systems*, vol. 62, pp. 868-878, 2014.

[9] K. E.Okedu, "Stability Enhancement of DFIG-based Variable Speed Wind Turbine with a Crowbar by FACTS Device as Per Grid Requirement,"*International Journal of Renewable Energy Research (IJRER)*, vol. 2, no 3, pp. 431-439, 2012.

[10] M.Rahimi, M.Parniani, "Grid-fault ride-through analysis and control of wind turbines with doubly fed Induction generators,"*Electric Power Systems Research*, vol. 80, pp.184-195, 2010.

[11] T. K. A. Brekken, N. Mohan, "Control of a doubly fed induction wind generator under unbalanced grid voltage conditions,"*IEEE Trans. on Energy Conversion*, vol. 22, no. 1,pp. 129-135, 2007.

[12] J.Yao, H. Li, Y. Liao, Z. Chen, "An improved control strategy of limiting the DC link voltage fluctuation for a Doubly Fed Induction wind generator,"*IEEE Trans. Power Electron*, vol. 23, no 3, pp. 1205-1213, 2008.

[13] A. G.Aissaoui, A.Tahour, M.Abid, N.Essounbouli, F.Nollet, M. I.Chergui, "Variable Structure Control Applied in Wind Turbine Based on Induction Generator,"*International Journal of Renewable Energy Research (IJRER)*, vol. 2, no. 4, pp. 600-607, 2012.

[14] Y.Bekakra, D. B.Attous, "Comparison Study between SVM and PWM Inverter in Sliding Mode Control of Active and Reactive Power Control of a DFIG for Variable Speed Wind Energy,"*International Journal of Renewable Energy Research (IJRER)*, vol. 2, no. 3, pp.471-476, 2012.

[15] M. Mohseni, M. A. Masoum, S. M. Islam, "Low and high voltage ride-through of DFIG wind turbines using hybrid current controlled converters,"*Electric Power Systems Research*, vol. 81, pp. 1456-1465, 2011.

[16] F. Hachicha, L. Krichen, "Rotor power control in doubly fed induction generator wind turbine under grid faults*," Energy*, vol. 44, pp. 853-861, 2012.

[17] N.Amuthan, P. Subburaj, P. Melba Mary, "Voltage sag ride through using improved Adaptive Internal Model Controller for doubly fed induction generator wind farms,"*Computers and Electrical Engineering*, vol. 39, pp. 214-224, 2013.

[18] K.Kerrouche, A. Mezouar, L. Boumedien, "A simple and efficient maximized power control of DFIG variable speed

wind turbine," *in Proceeding of IEEE 3rd International Conference Systems and Control (ICSC)*, (Algiers),pp. 894-899, 2013.

[19] T. R. Ayodele,A.Jimoh,J. L.Munda, A. J.Tehile, "Challenges of grid integration of wind power on power system grid integrity: a review,"*International journal of renewable energy research (IJRER)*, vol. 2, no 4, pp. 618-626, 2012.

[20] J. J.Justo, F.Mwasilu, J. W.Jung, "Doubly-fed induction generator based wind turbines: A comprehensive review of fault ride-through strategies,"*Renewable and Sustainable Energy Reviews*, vol. 45, pp.447-467, 2015.

[21] A. M.Howlader, T.Senjyu, "A comprehensive review of low voltage ride through capability strategies for the wind energy conversion systems,"*Renewable and Sustainable Energy Reviews*, vol. 56, pp. 643-658, 2016.

[22] M. M.Mansouri, M.Nayeripour, M.Negnevitsky, "Internal electrical protection of wind turbine with doubly fed induction generator,"*Renewable and Sustainable Energy Reviews*, vol. 55, pp. 840-855, 2016.

[23] J. J.Justo,K. S.Ro, "Control strategies of doubly fed induction generator-based wind turbine system with new rotor current protection topology,"*Journal of Renewable and Sustainable Energy*, vol. 4, no 4, 043123, 2012.

[24] J. J.Justo, F.Mwasilu, J. W.Jung, "Doubly fed induction generator wind turbines: A novel integrated protection circuit for low-voltage ride-through strategy*,"Journal of Renewable and Sustainable Energy*, vol. 6, no. 5, pp.053129, 2014.

[25] S. Bindeshwar, "Introduction to FACTS controllers in wind power farms: a technological review,"*International Journal of Renewable Energy Research (IJRER)*, vol. 2, no. 2, 2012.

[26] D. V. N.Ananth, G. N.Kumar, "Fault ride-through enhancement using an enhanced field oriented control technique for converters of grid connected DFIG and STATCOM for different types of faults," *ISA transactions*, 2015.

[27] A. F. Abdou, A.Abu-Siada,H. R. Pota, "Improving the low voltage ride through of doubly fed induction generator during intermittent voltage source converter faults*," Journal of Renewable and Sustainable Energy*, vol. 5, no. 4, pp. 043110, 2013.

[28] O. Abdel-Baqi, A.Nasiri, "Series voltage compensation for DFIG wind turbine low voltage ride-through solution,"*Energy Convers IEEE Trans*, vol. 26, pp. 272–280, 2011.

[29] D. Ramirez, S. Martinez, CA. Platero,F. Blazquez,RM. de Castro, "Low-voltage ride-through capability for wind generators based on dynamic voltage restorers,"*Energy Convers IEEE Trans*, vol. 26, pp. 195–203, 2011.

[30] S.Tohidi, M. I. Behnam, "A comprehensive review of low voltage ride through of doubly fed induction wind generators," *Renewable and Sustainable Energy Reviews*, vol. 57, pp. 412-419, 2016.

[31] R. M. Kamel, "Three fault ride through controllers for wind systems running in isolated micro-grid and Effects of fault type on their performance: A review and comparative study," *Renewable and Sustainable Energy Reviews*, vol. 37, pp. 698-714, 2014.

[32] J. Ouyang, X. Xiong, X. Zeng, "Analysis and evaluation of short-circuit current of doubly fed induction generation under rotor excitation control," *Journal of Renewable and Sustainable Energy*, vol. 6, no. 5, pp. 053128, 2014.

[33] M. Mohseni, S. Islam, MA. Masoum, "Fault ride-through capability enhancement of doubly-fed induction wind generators," *Renew Power Gener IET*, vol. 5, pp. 368–376, 2011.

[34] M.Mohseni, SM.Islam, "Transient control of DFIG-based wind power plants in compliance with the Australian grid code," *Power Electron IEEE Trans*, vol. 27, pp. 2813–24, 2012.

[35] Z. Li, S. C.Wong, X.Liu, Y.Huang, "Discrete Fourier series-based dual-sequence decomposition control of doubly-fed induction generator wind turbine under unbalanced grid conditions," *Journal of Renewable and Sustainable Energy*, vol. 7, no. 2, pp. 023130, 2015.

[36] K. D. E.Kerrouche, A.Mezouar, L. Boumediene, Kh. Belgacem, "Modeling and Optimum Power Control based DFIG Wind Energy Conversion System," *IREE*, vol. 9, no. 1, pp. 174 – 185, 2014.

[37] B. Robyns, B.Francois, P.Degobert, J. P, Hautier, *Vector control of induction machines*.London, England:Springer-Verlag, 2012.

[38] W.Ouled Amor, M. Ghariani, S.Guesmi, *"Supervision of a wind farm connected to the grid by the electric production distribution method," International Journal of Renewable Energy Research (IJRER)*, vol. 5, no. 4, pp. 944-951, 2015.

[39] PC.Krause,*Analysis of electric machinery*. New York, USA: McGraw Hill, 1986.

[40] J. J.Slotine, W.Li, *Applied non-linear Control*. New Jersey: Prentice-Hall Edition, 1991.

[41] V. I.Utkin, *Sliding Modes in Optimization and Control*. London, England: Springer-Verlag, 1992.

[42] A. Levant, "Sliding order and sliding accuracy in sliding mode control," *Int.J.Control*, vol. 58, no. 6, pp. 1247-1263, 1993.

[43] M. M. Rezaei, J. Soltani, "Sliding Mode Control of a Grid-Connected Distributed Generation Unit under Unbalanced Voltage Conditions," *Automatika Journal for Control, Measurement, Electronics, Computing and Communications*, vol. 60, no. 1, 2016.

[44] B.Beltran,T. Ahmed-Ali, and M.Benbouzid, *"High-Order Sliding-Mode Control of Variable-Speed Wind Turbines," IEEE Transactions on Industrial Electronics*, vol. 56, no. 9, pp. 3314 – 3321, 2009.

[45] A.Mezouar, M. K. Fellah, S. Hadjeri, "Robust sliding mode control and flux observer for induction motor using singular perturbation," *Electrical Engineering*, vol. 89, pp. 193-203, 2007.

[46] A.Djerioui, K.Aliouane, F.Bouchafaa, "Sliding Mode Observer of a Power Quality in Grid Connected Renewable Energy System,*International Journal of Renewable Energy Research (IJRER)*, vol. 2, no. 4, pp.541-548, 2012.

[47] A.Susperregui, G.Tapia, I. Zubia and. J. X. Ostolaza, "Sliding-mode control of doubly-fed generator for optimum power curve tracking,"*IET Electronics Letters*, vol. 46, no. 2, pp. 126-127, 2010.

[48] C.Evangelista, P.Puleston, F.Valenciaga, and L. M. Fridman, "Lyapunov-Designed Super-Twisting Sliding Mode Control for Wind Energy Conversion Optimization,"*IEEE Trans Industrial Electronics*, vol. 60, no. 2, 2013.

[49] F. Valenciaga,P. F. Puleston, "Variable structure control of a wind energy conversion system based on a brushless doubly fed reluctance generator,"*IEEE Trans Energy Convers*, vol. 22, no. 2, pp. 499-506, 2008.

[50] C.Evangelista, P. Puleston, F. Valenciaga, "Wind turbine efficiency optimization. Comparative study of controllers based on second order sliding modes,"*international journal of hydrogen energy*, vol. 35, pp. 5934-5939, 2010.

[51] L.Shang, D.Sun, J.Hu, "Sliding-mode-based direct power control of grid-connected voltage-sourced inverters under unbalanced network conditions,"*Power Electronics, IET*, vol. 4, no. 5, pp. 570-579, 2011.

[52] G.Abad, J.Lopez, M.Rodriguez, L.Marroyo, G.Iwanski, "Doubly fed induction machine: modeling and control for wind energy generation*,"John Wiley & Sons*, 2011.

[53] K.Ouaria, T. Rekioua, M. Ouhrouche, "Real time simulation of nonlinear generalized predictive control for wind energy conversion system with nonlinear observer,"*ISA Transactions*, vol. 53, pp. 76-84, 2014.

Kamel Djamel-Eddine Kerrouche was born in Saida, Algeria, in 1988. He received the B.S. and M.S. degrees in Electrical Engineering from Taher Moulay University, Saida, Algeria, in 2010 and 2012 respectively. He is currently a member of the Laboratory of Electrical Engineering, Taher Moulay University, Saida, Algeria, where he is preparing his Ph.D. His fields of interest are advanced control of electrical machines, power converters, modelling and control of wind turbines, improving grid power quality with FACTS device.

Abdelkader Mezouar was born in Mascara, Algeria, in 1974. He received the B.S. and M.S. degrees in Electrical Engineering from National Polytechnic School, Algiers, Algeria, in 1997 and 1999 respectively. Subsequently, he received the Ph.D. degree and the university habilitation from Djillali Liabes University, Sidi Bel Abbès, Algeria, in 2006 and 2008 respectively. He is currently a member of the Laboratory of Electrical Engineering, Taher Moulay University, Saida, Algeria. His research interests include electrical machines and drives, sliding mode control, observer techniques and renewable energy.

Larbi Boumediene is born in Saida (Algeria) in 1964. He obtained a diploma of engineer in Electrotechnics in 1990. He received his master Department of Electrical Engineering at the EN-SET, in Oran, Algeria. He received "Doctorate Es-Science" in Electrical Control from the University of Sciences and Technology of Oran (Algeria) in 2007. He is an associate professor at university of Saida. His fields of interest include harmonic power flow in distribution system and quality of energy.

Alex P. M. Van Den Bossche received the M.S. and the Ph.D. Degrees in electromechanical engineering from Ghent University Belgium, in 1980 and 1990respectively. He has worked there at the Electrical Energy Laboratory (EELAB). Since 1993, he is professor at the same university in the same field. His research is in the field of electrical drives, power electronics on various converter types and passive components and magnetic materials. He is also interested in renewable energy conversion. He is an author of the book Inductors and transformers for power electronics. He was a starter of two spin-off companies Invertor n.v. and Alenco n.v.

AUTHORS' ADDRESSES
Kamel Djamel Eddine,
School of Automation Science and Electrical Engineering,
Beihang University, Beijing 100091, China
Abdelkader Mezouar,
Larbi Boumediene,
Electro-technical Engineering Lab, Faculty of Technology,
Tahar Moulay University, Saida Algeria,
email: kerrouche20@yahoo.fr,
abdelkader.mezouar@univ-saida.dz,
larbi.boumediene@univ-saida.dz.

Alex P. M. Van Den Bossche,
Electrical Energy LAB EELAB,
Technologiepark 913 B 9052 Zwijnaarde, Ghent, Belgium
email: Alex.VandenBossche@ugent.be